Letter

Sequence-Specific Recognition of HIV-1 DNA with Solid-State CRISPR-Cas12a-Assisted Nanopores (SCAN)

Reza Nouri, Yuqian Jiang, Xiaojun Lance Lian,* and Weihua Guan*

Cite This: *ACS Sens.* 2020, 5, 1273−1280

Read Online

ACCESS | Metrics & More | Article Recommendations | SI Supporting Information

ABSTRACT: Nucleic acid detection methods are crucial for many fields such as pathogen detection and genotyping. Solid-state nanopore sensors represent a promising platform for nucleic acid detection due to its unique single molecule sensitivity and label-free electronic sensing. Here, we demonstrated the use of the glass nanopore for highly sensitive quantification of single-stranded circular DNAs (reporters), which could be degraded under the trans-cleavage activity of the target-specific CRISPR-Cas12a. We developed and optimized the Cas12a assay for HIV-1 analysis. We validated the concept of the solid-state CRISPR-Cas12a-assisted nanopores (SCAN) to specifically detect the HIV-1 DNAs. We showed that the glass nanopore sensor is effective in monitoring the cleavage activity of the target DNA-activated Cas12a. We developed a model to predict the total experimental time needed for making a statistically confident positive/negative call in a qualitative test. The SCAN concept combines the much-needed specificity and sensitivity into a single platform, and we anticipate that the SCAN would provide a compact, rapid, and low-cost method for nucleic acid detection at the point of care.

KEYWORDS: nanopores, CRISPR-Cas12a, HIV-1, point-of-care, diagnosis
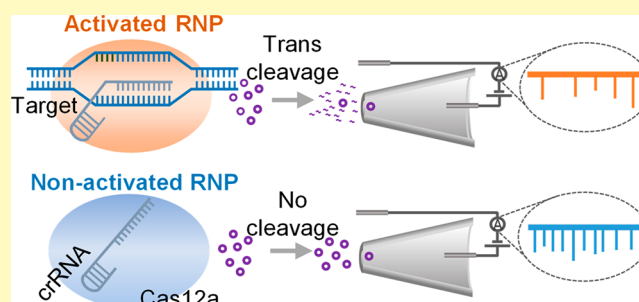
Solid-state nanopore sensors made from silicon nitride,[1−4] glass,[5−7] and graphene[8] have shown great potential in detecting single molecules due to their unique label-free electronic sensing, single molecule sensitivity, and potential reusability. In typical nanopore experiments, charged biopolymers such as DNAs are electrophoretically driven through the nanoscale orifice, which temporarily blocks the passage of ions that leads to a dip in the current. Each dip in the current indicates one translocation of the analyte through the nanopore, often called an event. The analysis of the event magnitude, shape, duration, and rate provides the basis for interpreting the molecule length, shape, charge, and concentration.[9] Thanks to its elegant concept, solid-state nanopores have achieved great success in analyzing macromolecules in the past decade. An existing common challenge for solid-state nanopores was the sensing specificity.[10] The typical approach for achieving the specificity is by specific binding sites on the nanopore wall surfaces[11,12] or using specific probe molecules.[13−15] Nevertheless, additional steps of surface functionalization could limit the device yield.[10] In addition, a specifically modified nanopore means that nanopore can only be used for a fixed target without being generally applicable.

The CRISPR-Cas9 system has shown outstanding competence in targeting nucleic acid with high specificity,[16,17] and has been explored by combining with the nanopore sensings.[18−20] In addition, the recent discovery of the collateral cleavage in other Cas proteins like Cas12 and Cas13 made it possible to translate the sequence-specific targeting to other

detectable signals, which has led to the increasing emergence of CRISPR-mediated biosensors.[17,21−27] For instance, Zhang and colleagues developed SHERLOCK (specific high sensitivity enzymatic reporter unlocking), which used RNA-guided RNases Cas13a or Cas13b for RNA detection.[23,24] In addition, RNA-guided DNase Cas12 was explored for DNA detection, generating multiple versatile systems such as HOLMES,[25] DETECTOR,[26] and Cas12aVDet.[27] These successes have immensely expanded the applicability of CRISPR/Cas systems for highly specific nucleic acid analysis. So far, most of the CRISPR-mediated biosensing applications used fluorescent, bioluminescent, or colorimetric reporters for readouts, which often require optical sensing and additional design and synthesis of reporter molecules like fluorescence/quencher beacons or gold nanoparticles.

In this work, we combined the high specificity offered by the Cas12a and high sensitivity offered by the glass nanopore sensor toward an electronic sensing platform for sequence-specific HIV-1 DNA detection. Cell-associated HIV DNA (CA-HIV DNA, which can be extracted from easily obtainable
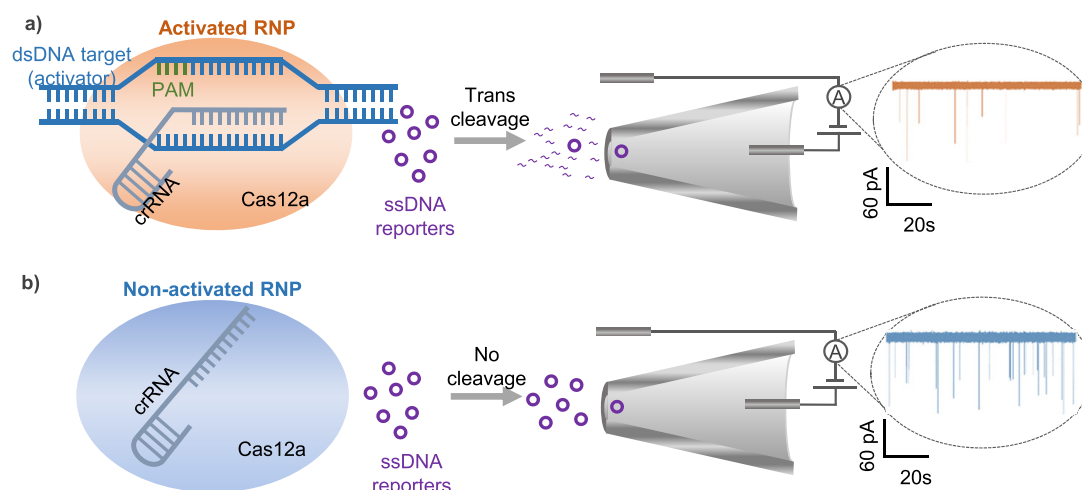
Figure 1. Schematic of solid-state CRISPR-Cas12a-assisted nanopore (SCAN) sensor. (a) Positive case, the trans-cleavage activity of the Cas12a after activation causes degradation of the circular ssDNA reporters, resulting in reduced reporter event rate through the nanopore. (b) Negative case, the Cas12a is not activated in the absence of target dsDNA and thus the ssDNA reporters are not cleaved. The nanopore event rate remains high.
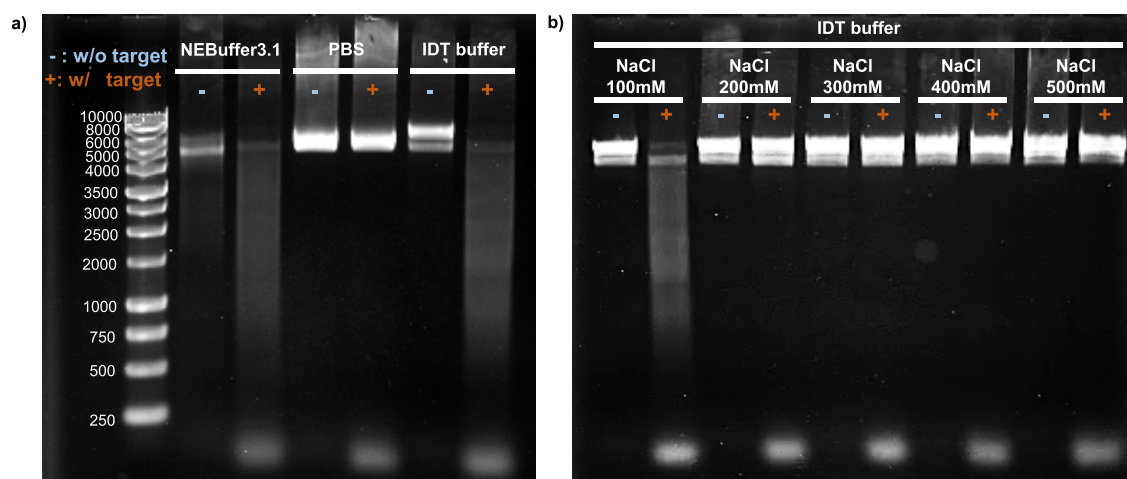

Figure 2. Buffer optimization for HIV-1 Cas12a assay. (a) Evaluating three candidate buffers: NEBuffer 3.1, PBS buffer, and IDT buffer (see SI Table S1 for detailed compositions). (b) Evaluating the impact of salt concentration on the Cas12a activity in the IDT buffer.

fingerprick blood) is the most widely used marker for HIV persistence in infected cells, the detection of which has significant importance in the diagnosis of HIV infection.[28] The solid-state CRISPR-Cas12a-assisted nanopores (SCAN) use circular single-stranded DNAs (ssDNAs) as reporters, which are cleavable when the crRNA/Cas12 complex (a.k.a., ribonucleoprotein or RNP) is activated by the binding of the specific HIV-1 DNA. We developed Cas12a assay for HIV-1 detection and optimized the buffer conditions for nanopore sensing. We found that the cleavage activity of the target DNA activated RNP can be quantified by the glass nanopore sensors. A model was developed to estimate the optimized reaction time and nanopore reading time such that positive/negative calls in a qualitative test at the 95% confidence level can be made as quickly as possible. We also validated the specificity of the SCAN for detecting two different regions of the HIV-1 gene. With excellent specificity and sensitivity, we believe SCAN offers a promising approach toward developing compact, rapid, and low-cost nucleic acid detection at the point of care.

■ RESULTS AND DISCUSSION

Working Principle. Figure 1 illustrates the working principle of SCAN for sequence-specific DNA detection. It leverages the unique features of the CRISPR-Cas12a and the nanopore sensor. Upon the specific RNA-guided dsDNA binding, the Cas12a could perform collateral cleavage on the surrounding nonspecific ssDNAs. This feature has been previously utilized for developing diagnostic tools.[22,25−27,29] In SCAN, circular ssDNAs (M13mp18, 7249 bases) of a known concentration (typically 100 pM) were used as reporters. If target HIV-1 DNAs exist in the analyte solution (Figure 1a), the Cas12a/crRNA complex (i.e., nonactivated RNP) can be activated by binding specifically to the target HIV-1 DNAs. The activated RNP was then able to digest the ssDNA reporters. During this process, the effective concentration of the circular ssDNA reporter was reduced. On the other hand, if the target HIV-1 DNAs do not present in the analyte solutions (Figure 1b), the RNP complex remains inactive and will not degrade the ssDNA reporter. As a result, the abundance of the remaining circular ssDNA reporter indicates the existence/absence of the target DNAs. The

SCAN approach used the glass nanopores for electronic quantification of the remaining ssDNA reporter through the single molecule counting.[7,30,31] The existence of the target HIV-1 DNAs would significantly reduce the ssDNA reporter event rate through the nanopore sensors. It is noteworthy that while the remaining ssDNA reporter can be readily visualized by conventional gel electrophoresis, the nanopore readout is much more sensitive and can be performed in situ (Supporting Information (SI) Figure S1). Due to the superior single molecule sensitivity of the nanopore, the ssDNA reporter concentration we used in SCAN (typically 100 pM) is much smaller than that in fluorescent platforms (typically 100 nM).

To ensure that all events observed in the nanopore sensors correspond to the ssDNA reporter rather than the interfering background molecules (e.g., RNPs), we performed nanopore experiments for a pure RNP and HIV-1 DNA sample (30 nM each) without any ssDNA reporter. We did not observe a single event for a measurement time of 1000 s (SI Figure S2), which confirms that the translocation rate of the background activated RNPs is less than 0.001 s^{-1}. The lack of signals from RNPs is most likely due to the fact that the size of the RNP complex and target DNA is much smaller than the circular reporter ssDNAs (7249 bases), which cannot be picked up by the large nanopores of a diameter of 10 nm.

HIV-1 Assay and Buffer Optimization. For sequence-specific recognition of HIV-1 DNA, the crRNAs should target conserved regions in all HIV-1 subtypes. To this end, we focused on three commonly evaluated domains of HIV-1, which are GAG (capsid protein), POL (protease, reverse transcriptase and integrase), and ENV (glycoprotein).[32−34] Based on these conservation in HIV gene sequences we synthesized two 50 bp dsDNAs from the GAG region as our HIV-1 targets. Two specific crRNAs were designed for each of these dsDNAs targets (see Methods for detailed sequences).

Toward a glass nanopore compatible reaction buffer,[18,19] we explored three candidates: NEBuffer 3.1, PBS buffer, and IDT buffer (see SI Table S1 for detailed compositions). The gel analysis was performed to validate each of these buffers (Figure 2a). As shown, the commonly used NEBuffer 3.1[25,27,35] indeed worked in our HIV-1 Cas12a assay. However, it is incompatible with the nanopore sensor. The presence of highly concentrated (1.5 μM) bovine serum albumin (BSA) in the NEBuffer acts as an opposing obstacle for ssDNA reporters and dramatically impact the nanopore ssDNA reporter event rates. For the PBS buffer, the gel results showed that it did not support the cleavage activity of Cas12a. This is likely due to the lack of Mg^{2+} ions, the key cofactor in Cas12a enzymatic activities.[36]

We hypothesized that a buffer with Mg^{2+} ions that has no BSAs is desirable for the SCAN device. The IDT buffer is such a candidate. We validated its functionality for our HIV-1 Cas12a assay (Figure 2a). While Cas12a indeed functioned properly in the IDT buffer, the low salt concentration of the buffer (100 mM) is nonideal for the nanopore sensing.[37] It was previously shown that high salt concentration would be favorable for nanopore sensing, as the low salt concentration will result in a dramatic reduction of event rate and the signal in glass nanopores.[30,38] To this end, we evaluated how increasing the salt concentration in the IDT buffer would impact the Cas12a assay. It was found that 200 mM salt would start killing the activity of the Cas12a (Figure 2b). This indicates that the IDT buffer with 100 mM salt should be used in the HIV-1 Cas12a reaction. To solve the conflicting buffer

requirements in the Cas12a reaction (low salt) and the nanopore sensing (high salt), we used a two-step protocol in our SCAN system. The reaction between the target DNA, Cas12a/crRNA, and ssDNA reporter was performed in the IDT buffer. The reaction was then terminated by adding 1.045 M KCl solution such that the final salt concentration is 1 M for efficient nanopore counting of the remaining ssDNA reporter.

Nanopore Event Rate for Circular ssDNA Reporter Quantification. For a typical SCAN experiment, the RNP concentration remains constant during the Cas12a cleavage reaction. To validate if the nanopore event rate can be used as a quantitative readout for the ssDNA reporter concentration at the constant RNP background, we performed nanopore counting experiments with serially diluted ssDNA reporter. In all experiments, the RNP and salt concentration was fixed as 30 nM and 1 M, respectively. Figure 3a shows the time traces
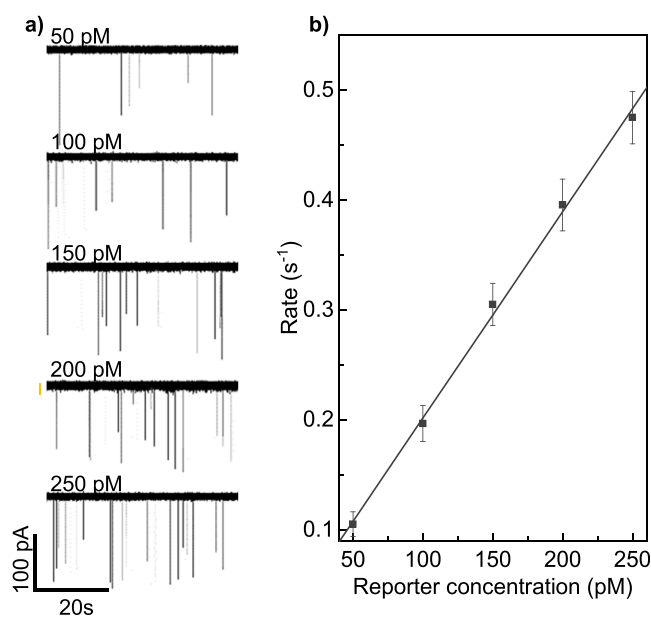

Figure 3. Quantitative ability at constant RNP concentrations. (a) Translocation recording of serially diluted ssDNA reporters ranging from 50 to 250 pM through the glass nanopore under 400 mV bias. The RNP and buffer salt concentration was fixed as 30 nM and 1 M, respectively. (b) Nanopore event rate as a function of the ssDNA reporter concentrations. The error bars correspond to the Poisson noise of determining the event rate.

of the ionic current from each of these cases. A quick glance of these traces revealed that events occur more often as the ssDNA reporter concentration increases. The extracted event rate as a function of the reporter concentration was plotted in Figure 3b. A clear linear relationship between the event rate and the ssDNA reporter concentration was observed (R^2 = 0.98), which validates that the abundance of ssDNA reporter can be quantified by nanopore counting at the constant RNP background.

HIV-1 Activated Cas12a Trans-Cleavage Monitored by Nanopore Counting. After verifying the linear relationship between the ssDNA reporter and the nanopore event rate under the constant RNP, we set out to perform HIV-1 sensing using the SCAN. Three different HIV-1 concentrations (15, 30, and 60 nM) were tested by adding the dsDNA sample to the RNP solutions in the IDT buffer. In all the experiments, the initial ssDNA reporter concentration was fixed at 100 pM.

The reaction was terminated at various reaction times (0, 5, 10, 20, and 30 min) by adding KCl salt to the final salt concentration of 1 M. The remaining ssDNA reporter concentration was measured by the calibration-free nanopore counting method[31] (SI Note S1).

Figure 4 plots the remaining ssDNA reporter concentration as a function of the reaction time for different target HIV-1
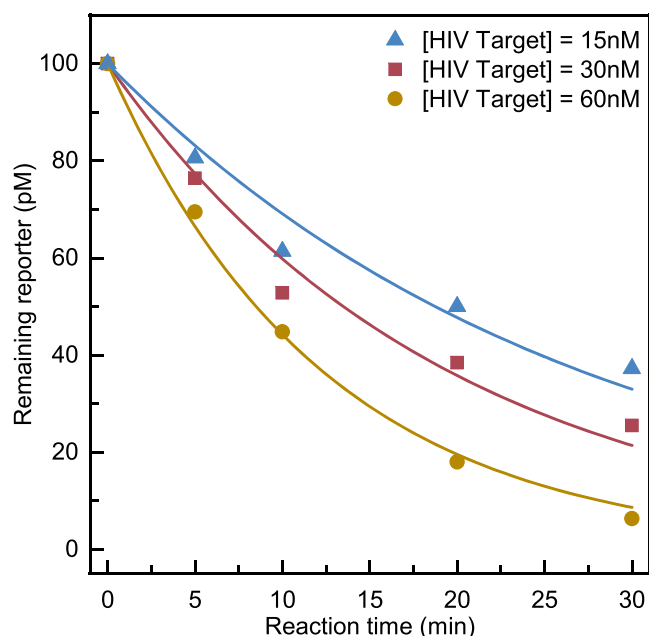

Figure 4. Remaining ssDNA reporter concentration as a function of reaction time (0, 5, 10, 20, and 30 min) for different HIV target concentrations (15, 30, and 60 nM). In each case, the initial ssDNA reporter concentration was set as 100 pM and the remaining concentration was obtained using the extracted translocation rate through the nanopore. The solid line is the fitting using the Michaelis–Menten kinetics, $C = C_0 \, e^{-kT_r}$, where C_0 is the initial ssDNA reporter concentration (100 pM). The fitted rate constants k for 15, 30, and 60 nM target HIV were obtained as 0.037, 0.051, and 0.081 min^{-1}, respectively.

concentrations. For each target HIV-1 concentration, the ssDNA reporter concentration reduced exponentially and can be fitted by the Michaelis–Menten kinetics, $C = C_0 \, e^{-kT_r}$, where C and C_0 are the remaining and initial ssDNA reporter concentration, respectively. T_r is the reaction time and k is the rate constant. The rate constant k went up from 0.037 min^{-1} at 15 nM target HIV to 0.051 min^{-1} at 30 nM target HIV, and further to 0.081 min^{-1} at 60 nM target HIV. These trans-cleavage rate constants were on par with previously reported value of 0.03 min^{-1}.[39] It was evident that the more target HIV-1 present in the analyte solution, the faster the ssDNA reporters are degraded by the activated Cas12a.

Although some of the translocation events recorded in the nanopore sensing could come from the partially cleaved ssDNA reporter, the fact that the remaining reporter extracted decayed exponentially by the reaction time (Figure 4) and followed the Michaelis–Menten kinetics suggested that the interference from the partially cleaved ssDNA reporter is negligible. To further explore the impact of the partially cleaved DNAs, we evaluated the distributions of the current dips, dwell time, and event charge deficits (ECDs) of the events for a negative sample and positive samples (SI Figure

S3). No significant difference was observed between these two samples, indicating that most of the detected events were from the intact circular ssDNA reporter.

Statistical Modeling for Qualitative Positive/Negative Test in SCAN. Practically, the SCAN device would require a certain reaction time T_r such that the HIV-1 activated Cas12a could degrade a certain amount of ssDNA reporters. The longer the reaction time, the fewer the remaining reporters. Subsequently, the remaining reporters will be measured by nanopore counting within a measurement time of T_m. It was previously shown that the translocation of molecules through the nanopore is a Poisson process.[40] Thus, inferring the event rate from observing n events in T_m will have an uncertainty of $(1.96(n)^{1/2})/T_m$.[41] In other words, longer measurement is statistically beneficial for more accurate rate determination. As a result, longer reaction time T_r and measurement time T_m is preferred to make a statistically confident call for a qualitative positive/negative test. However, minimizing the total experimental time ($T_r + T_m$) would be highly desirable toward a fast sample-to-result turnaround.

In order to estimate the total experimental time for a qualitative positive/negative test, we developed a statistical model. For the negative case (i.e., no reporter degradation), the expected number of events in the nanopore in a measurement time of T_m is given by

$$\lambda_n = \alpha \mu C_0 T_m \tag{1}$$

where μ is the electrophoretic mobility of the ssDNA reporter, α is a constant, and C_0 is the initial ssDNA reporter concentration before the reaction. On the other hand, for the positive case after reaction time T_r, the initial reporter concentration C_0 would decrease to $C_0 \, e^{-kT_r}$ (Michaelis–Menten kinetics) and the expected number of events in the nanopore in a measurement time of T_m would be

$$\lambda_p = \alpha \mu \, C_0 e^{-kT_r} T_m \tag{2}$$

in which k is the rate constant that is linearly proportional to the activated RNP concentration. The activated RNP concentration is limited by the smaller values between HIV-1 DNA and RNP concentration in the system and can be written as

$$k = A \times \min(C_{HIV}, C_{RNP}) \tag{3}$$

where A is a constant (0.00148 min^{-1} nM^{-1}; see SI Note S2).

In our experiment, we found that while the RNP complexes do not produce measurable events, they do affect the electrophoretic mobility of the ssDNA reporters. It was found that the reporter electrophoretic mobility is reduced exponentially as we increase the RNP concentration (SI Note S3). This phenomenon was previously observed in gel electrophoresis and was described by the Ogston–Morris–Rodbard–Chrambach model, in which molecule electrophoretic mobility has an exponential relationship with the obstacle concentration ($\mu \propto e^{-C_{RNP}}$).[42,43] Hence, electrophoretic mobility of the reporters can be extracted by fitting an exponential curve to our experimental results

$$\mu = \mu_0 \, e^{-\beta C_{RNP}} \tag{4}$$

where μ_0 (1.73 × 10^{-8} m^2 V^{-1} s^{-1}) and β (0.025 nM^{-1}) are the constants of the fitted exponential curve to the experimental results (SI Note S4).

Experimentally observed events for negative and positive cases would follow the Poisson distribution with expected values of λ_n and λ_p, respectively. As illustrated in Figure 5a, we
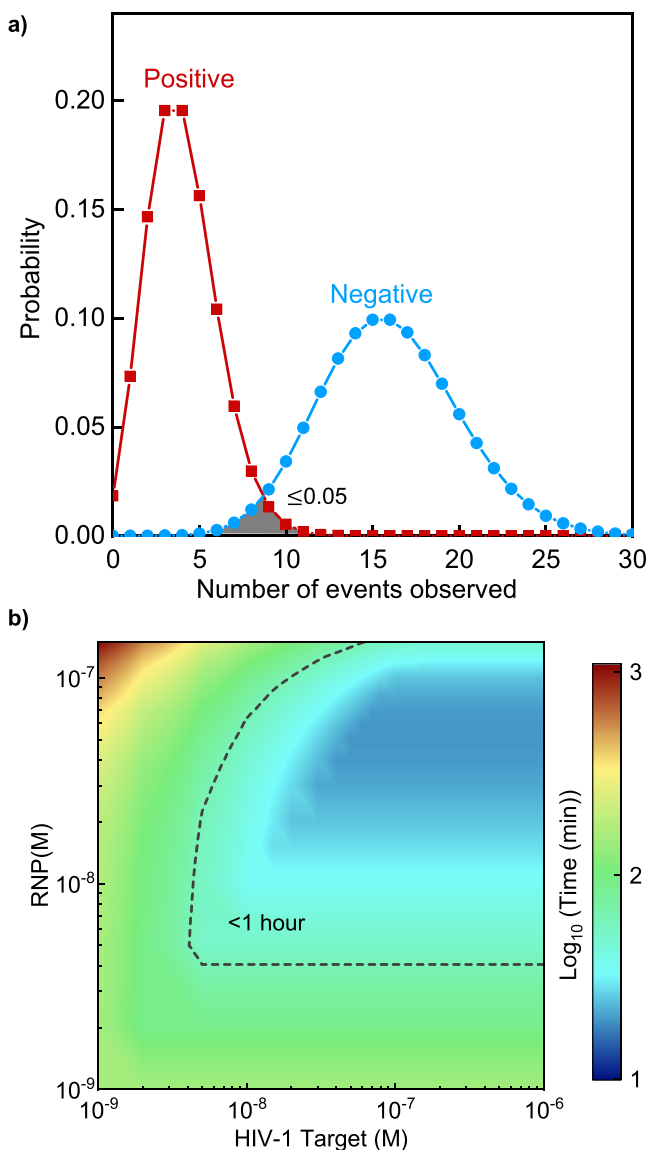

Figure 5. (a) Illustration of distributions for event numbers observed in the negative and positive case. The overlap of the two distributions should be less than 5% for a positive/negative call at the 95% confidence level. (b) Total experimental time needed for making a positive/negative call at different combinations of HIV target and RNP concentrations. The dashed−dotted line indicates the region in which the qualitative call can be made within 1 h.

aim to find out the λ_p such that the overlap of Poisson probability density functions (PDF) to that of the negative case of λ_n is less than 5% (i.e., 95% confidence level for making a positive/negative call). For any fixed nanopore reading time T_m, we can solve the maximal λ_p and therefore the minimal required reaction time T_r. Figure 5b plots the total experimental time $(T_r + T_m)$ as a function of HIV and RNP concentrations. We observed three important features. First, under a fixed RNP concentration, the total experimental time can be significantly reduced when the HIV target concentration is increased up to that of RNP concentration, beyond which the total experimental time is independent of the HIV-1

target concentration. This is because the rate constant k is determined by the smaller amount between target HIV-1 and RNP. Second, although in regions where RNP concentration is higher than HIV-1, the constant rate k is independent of RNP concentration, the total experimental time would be significantly increased when RNP target concentration is increased, especially more than 50 nM regions. This stems from the fact that the electrophoretic mobility of the reporters decays exponentially as we increase the RNP concentration (eq 4). Hence, we need more time in the nanopore reading to make a call at 95% confidence. Third, an optimized combination of HIV-1 and RNP concentration is required such that a positive/negative call at 95% confidence can be made within an hour (dashed line). It was found that the RNP concentration between 10 and 100 nM and HIV target concentration higher than 10 nM would be the optimized range in our experiment. If the starting HIV-1 DNA concentration is less than 10 nM, a preamplification step before SCAN is highly desirable for quick turnaround. These preamplification steps were widely used in previous Cas12a based assays.[26,27,29]

Sequence-Specific Test. We designed two sets of HIV-1 DNA targets and assays, in which each assay was specific to its target (Assay 1 to Target 1 and Assay 2 to Target 2). To test the cross-reactivity of designed assays, we performed the gel analysis on the assay products. Figure 6a showed the gel image. We observed clear reporter cleavage when the assays were used to their specific target, and no reporter cleavage if the assay is nonspecific to the target. To validate the specificity of the SCAN, we tested four different assay−target combinations. Figure 6b−e presents the results of the nanopore experiment before and after 30 min of reaction. For Target 1 in Assay 1, the translocation event rate change is significant (from 0.329 ± 0.036 s^{-1} to 0.128 ± 0.022 s^{-1}), whereas for Target 1 in Assay 2, the event rate change is negligible (from 0.271 ± 0.034 s^{-1} to 0.258 ± 0.032 s^{-1}). Similarly, for Target 2 in Assay 1, the translocation event rate change is negligible (from 0.310 ± 0.035 s^{-1} to 0.308 ± 0.039 s^{-1}), whereas for Target 2 in Assay 2, the translocation event rate change is significant (from 0.326 ± 0.037 s^{-1} to 0.103 ± 0.022 s^{-1}). It is clear that only the matched Cas12a assay and its target can produce a significant reduction in the number of translocation events after 30 min of reaction. These results demonstrated the SCAN could detect targets specifically. While nanopore sensors were often challenged by the specificity issue, we believe coupling the extremely high specificity of CRISPR Cas 12a to the nanopore sensor can provide an appealing alternative for future applications.

■ CONCLUSIONS

In summary, our findings demonstrated the capabilities of solid-state CRISPR-Cas12a-assisted nanopores for highly sensitive and specificity HIV-1 DNA detection. We found that the buffer salt concentration plays a critical role in both the assay and nanopore readout. We verified the events observed in the nanopore sensors were dominated by the uncleaved circular ssDNA reporter, rather than the background interference. The nanopore translocation event rate is a valid readout for quantifying the ssDNA reporters in the presence of the RNP complexes. We found that the reporter cleavage rate constant is proportional to the target HIV-1 concentration. We developed a model to estimate the optimized reaction time and nanopore reading time such that positive/negative calls in a qualitative test at the 95% confidence level can be made as
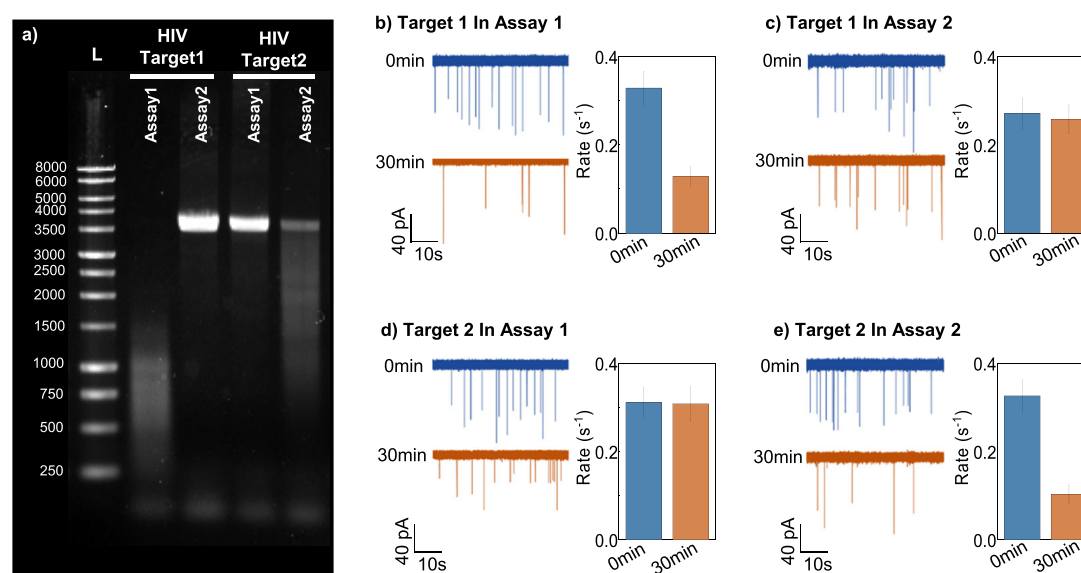
Figure 6. (a) Agarose gel electrophoresis images of the designed specificity test. Only specific combinations (Assay 1−Target 1 and Assay 2−Target 2) lead to the degradation of reporters. (b−e) Specificity test in SCAN. The reaction time for all cases is 30 min and the HIV target concentration is 30 nM. Only matched Cas12a assay and its target can produce a significant reduction in the number of translocation events. The error bars correspond to the Poisson noise of determining the event rate.

quickly as possible. We found that SCAN can detect target DNA concentrations above 10 nM within 1 h. Concentrations less than 10 nM would likely require preamplification steps, similar to previous Cas12a based assays.[26,27,29] We also validated the specificity of the SCAN for detecting two different regions of the HIV-1 gene. While the results presented in this work were from glass nanopores and HIV-1 DNAs, the SCAN principle could be extended to other nanopore types and DNA targets. We anticipate that SCAN would provide a new avenue for molecular diagnostic applications.

■ METHODS

Materials and Chemicals. A.s.Cas12a Ultra (#10001272) and IDTE pH7.5 buffer (#11-01-02-02) were purchased from Integrated DNA Technologies (IDT). dsDNA and crRNA were also synthesized from IDT. M13mp18 ssDNA (#N4040S) and NEBuffer 3.1 (#B7203S) were purchased from NEW ENGLAND Biolabs Inc. (NEB). DNA elution buffer was from Zymo Research (#D4036-5). Nuclease-free molecular Biology grade water was from Hyclone (SH30538). DPBS was purchased from Thermo Fisher (#14190250). DNA gel loading dye (6×) was from Thermo Fisher (#R0611). 10× IDT reaction buffer (200 mM HEPES, 1 M NaCl, 50 mM MgCl$_2$ and 1 mM EDTA, pH 6.5 @25 °C) was made at the lab. MgCl$_2$, NaCl, KCl, and Tris-EDTA-buffer solution (10 mM Tris-HCl and 1 mM EDTA) were purchased from Sigma-Aldrich. HEPES was from Gibco #15630-080. Agarose was from Biorad (#1613102). Ethidium bromide (EB) was from Life Technologies (#15585011). DNA ladder was from Thermo Scientific (#SM0311). Ag/AgCl wires electrodes were fabricated by using 0.2 mm Ag wires (Warner Instruments, Hamden, USA). Micro injectors of 34 gauge were purchased from World Precision Instruments. Piranha solution was made by mixing concentrated sulfuric acid (H$_2$SO$_4$) with hydrogen peroxide (H$_2$O$_2$). Quartz capillaries with inner and outer diameter of 0.5 mm and 1 mm were purchased from Sutter Instrument.

HIV-1 Cas12a Assay. Aligned sequences of three domains of HIV-1, which are GAG (capsid protein), POL (protease, reverse transcriptase, and integrase), and ENV (glycoprotein) were from HIV sequence database.[28] The Shannon entropy value of each nucleotide of the aligned sequences was calculated with the "Entropy-One" function in the HIV sequence database. Two HIV-1 DNA oligos from

the GAG region (HIV-1 Target 1 and Target 2) and two specific crRNAs were synthesized by IDT. Sequences are as follows.

Target 1: 5′-tatcacctagaac<u>TTTA</u>AATGCATGGGTAAAAG-TAGTAgaagagaaggct-3′

crRNA1: 5′-UAAUUUCUACUCUUGUAGAUAAUGCAUGGG-UAAAAGUAGUA-3′

Target 2: 5′-cc<u>TTTA</u>ACTTCCCTCAGGTCACTCTTTGGcaac-gacccctcgtcacaataa-3′

crRNA2: 5′-UAAUUUCUACUCUUGUAGAUACUUCCC-UCAGGUCACUCUUUGG-3′

The synthesized HIV-1 DNA oligos were resuspended in molecular biology grade water, annealed in DNA elution buffer. The crRNAs were resuspended in IDTE pH 7.5 buffer and stored in −80 °C. For RNP formation, Cas12a and crRNA were mixed in 1 × PBS to form the nonactivated RNP at room temperature for 20 min and stored in −80 °C. In the cleavage reaction, nonactivated RNP complex was mixed with dsDNA target and incubated at 37 °C for 10 min for RNP activation. Then, ssDNA reporters were added and incubated at 37 °C for cleavage. After the reaction, results were examined both in agarose gel and in the nanopore device. For gel imaging, reactions were terminated with DNA loading dye (6×). The 24 μL mixture was loaded to EB-stained 1% (wt/vol) agarose gel for electrophoresis analysis. For nanopore analysis, reactions were terminated by adjusting the salt concentrations to 1 M KCl.

Glass Nanopore Fabrication. To remove organic residues from quartz capillaries, as-purchased quartz capillaries were first cleaned in Piranha solution for 30 min, then rinsed with DI water, and dried in a vacuum oven at 120 °C for 15 min. A two-line recipe, (1) Heat 750, Filament 5, Velocity 50, Delay140, and Pull 50; (2) Heat 710, Filament 4, Velocity 30, Delay 155, and Pull 215, was used to pull the capillaries with a laser pipet puller (P-2000, Sutter Instruments, USA). This recipe typically produces nanopores of diameter around 10 nm. It is noteworthy that ssDNA that is less than 1 kbp in length does not generate detectable signal in the glass nanopore.

Nanopore Sensing and Data Analysis. A constant voltage was applied across the glass nanopore by 6363 DAQ card (National Instruments, USA). A trans-impedance amplifier (Axopatch 200B, Molecular Device, USA) was used to amplify the resulting current and then digitized by the 6363 DAQ card at 100 kHz sampling rate. Finally, a customized MATLAB (MathWorks) software was used to analyze the current time trace and extract the single molecule translocation information.

■ ASSOCIATED CONTENT

Ⓢ Supporting Information

The Supporting Information is available free of charge at https://pubs.acs.org/doi/10.1021/acssensors.0c00497.

Comparison between the sensitivity of traditional gel electrophoresis and nanopore sensor, nanopore experiment results for pure RNP sample with no reporter. Detailed descriptions of linking ssDNA reporter concentration with translocation rate, Michaelis−Menten kinetics, and Ogston-Morris-Rodbard-Chrambach (OMRC) model. Detailed compositions of NEBuffer 3.1, PBS buffer, and IDT buffer. (PDF)

■ AUTHOR INFORMATION

Corresponding Authors

Xiaojun Lance Lian − *Department of Biomedical Engineering, Huck Institutes of the Life Sciences, and Department of Biology, Pennsylvania State University, University Park, Pennsylvania 16802, United States*; Email: Lian@psu.edu

Weihua Guan − *Department of Electrical Engineering and Department of Biomedical Engineering, Pennsylvania State University, University Park, Pennsylvania 16802, United States*; ⓞ orcid.org/0000-0002-8435-9672; Email: w.guan@psu.edu

Authors

Reza Nouri − *Department of Electrical Engineering, Pennsylvania State University, University Park, Pennsylvania 16802, United States*

Yuqian Jiang − *Department of Biomedical Engineering and Huck Institutes of the Life Sciences, Pennsylvania State University, University Park, Pennsylvania 16802, United States*

Complete contact information is available at:
https://pubs.acs.org/10.1021/acssensors.0c00497

Author Contributions

R.N. and Y.J. contributed equally to the work. R.N. performed the nanopore fabrication and sensing experiment. Y.J. developed the HIV-1 assay. W.G. conceived of the concept and together with X.L.L. supervised the study. All authors analyzed the data and cowrote the manuscript.

Notes

The authors declare no competing financial interest.

■ ACKNOWLEDGMENTS

■ REFERENCES

(1) Firnkes, M.; Pedone, D.; Knezevic, J.; Doblinger, M.; Rant, U. Electrically facilitated translocations of proteins through silicon nitride nanopores: conjoint and competitive action of diffusion, electrophoresis, and electroosmosis. *Nano Lett.* **2010**, *10* (6), 2162−2167.

(2) Li, J.; Gershow, M.; Stein, D.; Brandin, E.; Golovchenko, J. A. DNA molecules and configurations in a solid-state nanopore microscope. *Nat. Mater.* **2003**, *2* (9), 611−615.

(3) Smeets, R.; Kowalczyk, S. W.; Hall, A.; Dekker, N.; Dekker, C. Translocation of RecA-coated double-stranded DNA through solid-state nanopores. *Nano Lett.* **2009**, *9* (9), 3089−3095.

(4) Roshan, K. A.; Tang, Z.; Guan, W. High fidelity moving Z-score based controlled breakdown fabrication of solid-state nanopore. *Nanotechnology* **2019**, *30* (9), 095502.

(5) Steinbock, L. J.; Bulushev, R. D.; Krishnan, S.; Raillon, C.; Radenovic, A. DNA translocation through low-noise glass nanopores. *ACS Nano* **2013**, *7* (12), 11255−11262.

(6) Lan, W.-J.; Holden, D. A.; Zhang, B.; White, H. S. Nanoparticle transport in conical-shaped nanopores. *Anal. Chem.* **2011**, *83* (10), 3840−3847.

(7) Tang, Z.; Choi, G.; Nouri, R.; Guan, W. Loop-Mediated Isothermal Amplification-Coupled Glass Nanopore Counting Toward Sensitive and Specific Nucleic Acid Testing. *Nano Lett.* **2019**, *19* (11), 7927−7934.

(8) Garaj, S.; Hubbard, W.; Reina, A.; Kong, J.; Branton, D.; Golovchenko, J. Graphene as a subnanometre trans-electrode membrane. *Nature* **2010**, *467* (7312), 190−193.

(9) Miles, B. N.; Ivanov, A. P.; Wilson, K. A.; Doğan, F.; Japrung, D.; Edel, J. B. Single molecule sensing with solid-state nanopores: novel materials, methods, and applications. *Chem. Soc. Rev.* **2013**, *42* (1), 15−28.

(10) Keyser, U. F. Enhancing nanopore sensing with DNA nanotechnology. *Nat. Nanotechnol.* **2016**, *11* (2), 106.

(11) Iqbal, S. M.; Akin, D.; Bashir, R. Solid-state nanopore channels with DNA selectivity. *Nat. Nanotechnol.* **2007**, *2* (4), 243.

(12) Wei, R.; Gatterdam, V.; Wieneke, R.; Tampé, R.; Rant, U. Stochastic sensing of proteins with receptor-modified solid-state nanopores. *Nat. Nanotechnol.* **2012**, *7* (4), 257.

(13) Sze, J. Y.; Ivanov, A. P.; Cass, A. E.; Edel, J. B. Single molecule multiplexed nanopore protein screening in human serum using aptamer modified DNA carriers. *Nat. Commun.* **2017**, *8* (1), 1−10.

(14) Kong, J.; Zhu, J.; Keyser, U. F. Single molecule based SNP detection using designed DNA carriers and solid-state nanopores. *Chem. Commun.* **2017**, *53* (2), 436−439.

(15) Bell, N. A.; Keyser, U. F. Specific protein detection using designed DNA carriers and nanopores. *J. Am. Chem. Soc.* **2015**, *137* (5), 2035−2041.

(16) Cong, L.; Ran, F. A.; Cox, D.; Lin, S.; Barretto, R.; Habib, N.; Hsu, P. D.; Wu, X.; Jiang, W.; Marraffini, L. A. Multiplex genome engineering using CRISPR/Cas systems. *Science* **2013**, *339* (6121), 819−823.

(17) Qin, P.; Park, M.; Alfson, K. J.; Tamhankar, M.; Carrion, R.; Patterson, J. L.; Griffiths, A.; He, Q.; Yildiz, A.; Mathies, R. Rapid and fully microfluidic Ebola virus detection with CRISPR-Cas13a. *ACS sensors* **2019**, *4* (4), 1048−1054.

(18) Yang, W.; Restrepo-Pérez, L.; Bengtson, M.; Heerema, S. J.; Birnie, A.; van der Torre, J.; Dekker, C. Detection of CRISPR-dCas9 on DNA with solid-state nanopores. *Nano Lett.* **2018**, *18* (10), 6469−6474.

(19) Weckman, N. E.; Ermann, N.; Gutierrez, R.; Chen, K.; Graham, J.; Tivony, R.; Heron, A.; Keyser, U. F. Multiplexed DNA identification using site specific dCas9 barcodes and nanopore sensing. *ACS sensors* **2019**, *4* (8), 2065−2072.

(20) Bulushev, R. D.; Marion, S.; Petrova, E.; Davis, S. J.; Maerkl, S. J.; Radenovic, A. Single Molecule Localization and Discrimination of DNA−Protein Complexes by Controlled Translocation Through Nanocapillaries. *Nano Lett.* **2016**, *16* (12), 7882−7890.

(21) Li, Y.; Li, S.; Wang, J.; Liu, G. CRISPR/Cas systems towards next-generation biosensing. *Trends Biotechnol.* **2019**, *37* (7), 730−743.

(22) He, Q.; Yu, D.; Bao, M.; Korensky, G.; Chen, J.; Shin, M.; Kim, J.; Park, M.; Qin, P.; Du, K. High-throughput and all-solution phase African Swine Fever Virus (ASFV) detection using CRISPR-Cas12a and fluorescence based point-of-care system. *Biosens. Bioelectron.* **2020**, *154*, 112068.

(23) Gootenberg, J. S.; Abudayyeh, O. O.; Kellner, M. J.; Joung, J.; Collins, J. J.; Zhang, F. Multiplexed and portable nucleic acid

detection platform with Cas13, Cas12a, and Csm6. *Science* **2018**, *360* (6387), 439−444.

(24) Gootenberg, J. S.; Abudayyeh, O. O.; Lee, J. W.; Essletzbichler, P.; Dy, A. J.; Joung, J.; Verdine, V.; Donghia, N.; Daringer, N. M.; Freije, C. A. Nucleic acid detection with CRISPR-Cas13a/C2c2. *Science* **2017**, *356* (6336), 438−442.

(25) Li, S.-Y.; Cheng, Q.-X.; Liu, J.-K.; Nie, X.-Q.; Zhao, G.-P.; Wang, J. CRISPR-Cas12a has both cis-and trans-cleavage activities on single-stranded DNA. *Cell Res.* **2018**, *28* (4), 491−493.

(26) Chen, J. S.; Ma, E.; Harrington, L. B.; Da Costa, M.; Tian, X.; Palefsky, J. M.; Doudna, J. A. CRISPR-Cas12a target binding unleashes indiscriminate single-stranded DNase activity. *Science* **2018**, *360* (6387), 436−439.

(27) Wang, B.; Wang, R.; Wang, D.; Wu, J.; Li, J.; Wang, J.; Liu, H.; Wang, Y. Cas12aVDet: a CRISPR/Cas12a-based platform for rapid and visual nucleic acid detection. *Anal. Chem.* **2019**, *91* (19), 12156−12161.

(28) Rouzioux, C.; Avettand-Fenoël, V. Total HIV DNA: a global marker of HIV persistence. *Retrovirology* **2018**, *15* (1), 30.

(29) Li, S.-Y.; Cheng, Q.-X.; Wang, J.-M.; Li, X.-Y.; Zhang, Z.-L.; Gao, S.; Cao, R.-B.; Zhao, G.-P.; Wang, J. CRISPR-Cas12a-assisted nucleic acid detection. *Cell discovery* **2018**, *4* (1), 1−4.

(30) Nouri, R.; Tang, Z.; Guan, W. Quantitative Analysis of Factors Affecting the Event Rate in Glass Nanopore Sensors. *ACS sensors* **2019**, *4* (11), 3007−3013.

(31) Nouri, R.; Tang, Z.; Guan, W. Calibration-free nanopore digital counting of single molecules. *Anal. Chem.* **2019**, *91* (17), 11178−11184.

(32) Zhao, J.; Chang, L.; Wang, L. Nucleic acid testing and molecular characterization of HIV infections. *Eur. J. Clin. Microbiol. Infect. Dis.* **2019**, *38* (5), 829−842.

(33) Schlatzer, D.; Haqqani, A. A.; Li, X.; Dobrowolski, C.; Chance, M. R.; Tilton, J. C. A targeted mass spectrometry assay for detection of HIV gag protein following induction of latent viral reservoirs. *Anal. Chem.* **2017**, *89* (10), 5325−5332.

(34) Waheed, A. A.; Freed, E. O. HIV type 1 Gag as a target for antiviral therapy. *AIDS Res. Hum. Retroviruses* **2012**, *28* (1), 54−75.

(35) Huang, M.; Zhou, X.; Wang, H.; Xing, D. Clustered regularly interspaced short palindromic repeats/Cas9 triggered isothermal amplification for site-specific nucleic acid detection. *Anal. Chem.* **2018**, *90* (3), 2193−2200.

(36) Fuchs, R. T.; Curcuru, J.; Mabuchi, M.; Yourik, P.; Robb, G. B. Cas12a trans-cleavage can be modulated in vitro and is active on ssDNA, dsDNA, and RNA. *bioRxiv* **2019**, 600890.

(37) Chen, K.; Bell, N. A.; Kong, J.; Tian, Y.; Keyser, U. F. Direction-and salt-dependent ionic current signatures for dna sensing with asymmetric nanopores. *Biophys. J.* **2017**, *112* (4), 674−682.

(38) Ermann, N.; Hanikel, N.; Wang, V.; Chen, K.; Weckman, N. E.; Keyser, U. F. Promoting single-file DNA translocations through nanopores using electro-osmotic flow. *J. Chem. Phys.* **2018**, *149* (16), 163311.

(39) Strohkendl, I.; Saifuddin, F. A.; Rybarski, J. R.; Finkelstein, I. J.; Russell, R. Kinetic basis for DNA target specificity of CRISPR-Cas12a. *Mol. Cell* **2018**, *71* (5), 816−824.

(40) Meller, A.; Branton, D. Single molecule measurements of DNA transport through a nanopore. *Electrophoresis* **2002**, *23* (16), 2583−2591.

(41) Patil, V.; Kulkarni, H. Comparison of confidence intervals for the Poisson mean: some new aspects. *REVSTAT−Statistical Journal* **2012**, *10* (2), 211−227.

(42) Mercier, J.-F.; Slater, G. W. An exactly solvable Ogston model of gel electrophoresis. 7. Diffusion and mobility of hard spherical particles in three-dimensional gels. *Macromolecules* **2001**, *34* (10), 3437−3445.

(43) Slater, G. W.; Guo, H. L. Ogston gel electrophoretic sieving: How is the fractional volume available to a particle related to its mobility and diffusion coefficient (s)? *Electrophoresis* **1995**, *16* (1), 11−15.